



## Adsorption kinetics and optimum conditions for Cr(VI) removal by activated carbon prepared from luffa sponge

Ming-sheng Miao<sup>a</sup>, Yan-na Wang<sup>a</sup>, Qiang Kong<sup>a,\*</sup>, Li Shu<sup>b</sup>

<sup>a</sup>College of Life Science, Shandong Normal University, 88 Wenhua Donglu, Shandong, Jinan 250014, P.R. China, Tel. +86 531 86180745; Fax: +86 531 86180107; emails: [mingshengmiao@163.com](mailto:mingshengmiao@163.com) (M.-s. Miao), [1461187809@qq.com](mailto:1461187809@qq.com) (Y.-n. Wang), [kongqiang0531@hotmail.com](mailto:kongqiang0531@hotmail.com) (Q. Kong)

<sup>b</sup>School of Engineering, Faculty of Science, Engineering and Built Environment, Deakin University, Geelong, Victoria 3216, Australia, email: [li.shu846@gmail.com](mailto:li.shu846@gmail.com)

Received 28 November 2014; Accepted 24 January 2015

### ABSTRACT

Activated carbon (AC) prepared from luffa sponge was firstly used as an adsorbent to remove Cr(VI) from aqueous solution. The Cr(VI) adsorption behaviors of AC under different conditions, including initial Cr(VI) concentration, quantity of AC, solution pH, and temperature were investigated. The optimal conditions for adsorption of Cr(VI) by AC were pH = 1, initial Cr(VI) concentration = 80 mg/L,  $T = 303$  K, and AC content = 1.6 g/L. The adsorption kinetics could be described by the pseudo-second-order model. Fourier transform infrared spectroscopy was used to investigate the sorption mechanism. Some functional groups such as C–O and O–H were formed on the carbon surface, which could then react with Cr(VI). The surface structure of AC before and after adsorption was analyzed by scanning electronic microscopy. Adsorbed ions choked some of the pores in AC after adsorption. The Brunauer–Emmett–Teller surface area and average pore size of the AC were 834.13 m<sup>2</sup>/g and 5.17 nm, respectively. The maximum adsorption of Cr(VI) by AC was 149.06 mg/g, which makes AC prepared from luffa sponge promising for removing Cr(VI) from wastewater.

*Keywords:* Luffa sponge; AC; Cr(VI); Adsorption

### 1. Introduction

As a result of the rapid development of industry and technology, chromium has become widely distributed in the environment in its two common oxidation states of Cr(III) and Cr(VI). Cr(III) is an essential trace element, while Cr(VI) compounds are considered

highly toxic because of their carcinogenic, teratogenic, and mutagenic effects on humans and other living organisms [1]. Cr(VI) is widely present in the effluents of electroplating, metal finishing, leather tanning, and pigment industries. As a result, such effluents may pose a severe threat to public health and the environment if discharged without adequate treatment [2]. A variety of techniques, such as electrochemical

\*Corresponding author.

Presented at the 7th International Conference on Challenges in Environmental Science and Engineering (CESE 2014) 12–16 October 2014, Johor Bahru, Malaysia

treatment, coagulation/precipitation, membrane filtration, ion exchange, adsorption, and biological processes have been developed to remove Cr(VI) contaminants from wastewaters [3–7]. However, many of these processes are not widely practiced because of disadvantages, including incomplete metal removal, high cost, and generation of toxic sludge or other waste products that require disposal [8].

Activated carbon (AC) is widely used in an industrial scale as an adsorbent in purification and separation processes, as a catalyst or catalyst support in catalysis, and as an electrode material in electrochemical devices and processes because of its high specific surface area and relatively high mechanical strength [9]. Therefore, the demand for AC is continuously increasing [10].

However, commercially available AC is usually expensive because of its high-cost sources, and this restricts its extensive application [11]. Therefore, it is necessary to find a cheaper, more efficient substitute to produce AC. Researchers have prepared AC from sources, including bamboo, bagasse, walnut shells, nut shells, pine cones, peanut shells, cotton stalks, and tobacco residue [12–19] in attempts to produce low-cost, high-performance AC. There are also several raw materials, which were used to prepare adsorption carbon, that was used to adsorb Cr(VI) from the wastewater such as *Trapa natans* husk, peanut shells, and so on.

Luffa sponge is a commercially viable and biological material derived from fruit of the *Luffa cylindrica* plant that has recycling capability and biodegradability [20]. The dried fibrous part of the *L. cylindrica* is commonly used as a washing sponge and filter because of its fibrous vascular system.

In this work, AC prepared from luffa sponge was firstly used as an adsorbent to remove Cr(VI) from aqueous solution. Using phosphoric acid ( $\text{H}_3\text{PO}_4$ ) as a flame-retardant and activating agent in the preparation of ACs has been well established [21,22], therefore this method was chosen to prepare AC from luffa sponge. To investigate the adsorption mechanism of the AC, its superficial area, surface structure, pore-size distribution, and Fourier transform infrared (FTIR) spectrum were analyzed. Various parameters affecting adsorption Cr(VI) onto the prepared AC, such as initial concentration, the quantity of AC, solution pH, and temperature were studied. This work aimed to evaluate the potential of developing an effective low-cost adsorbent from luffa sponge by  $\text{H}_3\text{PO}_4$  activation and investigate its ability to treat wastewater containing toxic Cr(VI).

## 2. Materials and methods

### 2.1. Materials and chemicals

Luffa sponge was obtained from a local market in Jinan. After washing and drying, the sponge was crushed by a high speed grinder (HCP-100, Jinsui company, Zhejiang), and then activated by treatment in  $\text{H}_3\text{PO}_4$  (1 + 1) for 12 h, the solid to liquid ratio was 1:4–6 (g:mL). The sample was carbonized for 450 °C for 1 h, and then eluted with deionized water until the pH was nearly 7 before being dried in an oven for 12 h at 120 °C. A mortar was used to grind the AC to a particle size of 150–200 mesh. All chemicals used were of analytical grade. About 2.829 g of oven-dried  $\text{K}_2\text{Cr}_2\text{O}_7$  was dissolved in distilled water to bring the volume of the solution to 1,000 mL. This will produce a stock solution of 1,000 mg/L of Cr(VI), other concentrations were obtained by diluting the stock solution with distilled water.

### 2.2. Characterization of AC

The structural characteristics of the AC samples were investigated. Brunauer–Emmett–Teller (BET) specific surface areas were calculated based on  $\text{N}_2$  adsorption/desorption isotherms measured at 77 K using a surface area analyzer (Quantachrome, USA). Pore-size distribution and porosity were determined by a porosity analyzer (Quadrasorb SI, Quantachrome). Scanning electron microscopy (SUPRA™ 55, Zeiss Company, Germany) was used to observe the surface of the AC samples. FTIR spectra of AC before and after adsorption experiments were recorded in the range of 4,000–400  $\text{cm}^{-1}$  using an FTIR spectrometer (Thermo Scientific, USA).

### 2.3. Adsorption experiments

Batch Cr(VI) adsorption studies were performed by mixing a predetermined amount of AC with 50 mL of Cr(VI) solution at different concentration in 250 mL conical flasks. The flasks were shaken at 180 rpm in an oven-controlled crystal oscillator (HZQ-2, Jintan, Beijing), and the temperature was controlled at  $25 \pm 2$  °C for 3 h to achieve equilibrium. After 10 min standing, the supernate was removed, and then the residual Cr(VI) concentration was calculated according to a standard method, using a UV–vis spectrophotometer (T6-Xinshiji, Beijing) at a wavelength of 540 nm [1]. To study the effect of pH on the adsorption behavior of the AC, the initial solution pH was adjusted to 1–12

with phosphoric acid or NaOH solution. The pH values were measured by a pH meter (PHS-3D, China). Adsorption isotherm experiments were performed at 20, 30, and 40°C. The adsorption quantity  $Q_e$  (mg/g), and removal efficiency of Cr(VI) at equilibrium can be calculated as follows:

$$Q_e = (C_0 - C_e)V/W \quad (1)$$

$$\% \text{ removal} = 100(C_0 - C_e)/C_0 \quad (2)$$

where  $Q_e$  is the equilibrium Cr(VI) concentration (mg/L),  $C_0$  is the initial Cr(VI) concentration (mg/L),  $V$  is the solution volume (L), and  $W$  is the mass of adsorbent (g).

#### 2.4. Orthogonal experiment

Orthogonal experimental design is a method that has been used to study various factors and levels affecting experimental outcomes. Using a normal design of four factors and three levels, adsorption experiments were performed under different controlled conditions to determine optimal experiment conditions. The four factors were initial concentration, quantity of AC, solution pH, and temperature. The three levels were ascertained through initial experiments and a single-factor experiment.

#### 2.5. Adsorption kinetics

The adsorption kinetics of the AC for Cr(VI) were investigated. Pseudo-first-order kinetics is observed when the adsorption rate is influenced by solution concentration and adsorbance. The resistance of intraparticle mass transfer is the limiting factor of adsorption. In contrast, pseudo-second-order kinetics is observed when the limiting factor of the adsorption process is the adsorption mechanism rather than intraparticle mass transfer. Intraparticle diffusion is the controlling step in many adsorption processes. The pseudo-first-order and pseudo-second-order models as well as the intraparticle diffusion rate were used to analyze the adsorption kinetics of AC for Cr(VI).

### 3. Results and discussion

#### 3.1. Characteristics of AC

SEM was used to examine the surface characteristics of the virgin AC and Cr(VI)-adsorbed AC samples (Fig. 1). The surface of the AC before adsorption was porous (Fig. 1(a)). AC samples adsorbed with Cr(VI)

(Fig. 1(b)), the surface structure of the AC was coarse. As shown in the SEM, the abundant pore structures and high surface area made AC one of the most effective adsorption materials.

The pore-size distribution of the AC before adsorption is presented in Fig. 2 indicated the presence of micro-mesoporous structures with most pores <5 nm in diameter; the correlation coefficient was  $r = 0.9997$ . The  $N_2$  adsorption/desorption isotherms for AC (insert of Fig. 2) were consistent with a type-IV curve according to IUPAC classification. The BET surface area and average pore size of the AC were  $834.13 \text{ m}^2/\text{g}$  and 5.17 nm, respectively.

#### 3.2. Effect of contact time

To explore the adsorption equilibrium time of the AC for Cr(VI) removal, solutions containing initial chromium concentrations of 20 and 50 mg/L were prepared and mixed with 0.05 g of AC. Fig. 3 shows how Cr(VI) removal by the AC changed over time. The percentage of Cr(VI) removed increased rapidly during the first 30 min for all concentrations, and then gradually slowed. After 180 min, the removal rate tended toward stability. The rapid initial increase was probably caused by the abundant bonding sites of AC and large concentration gradients existing between Cr(VI) in aqueous and solid phases [11]. The adsorption of Cr(VI) by AC depended on the initial concentration of Cr(VI). The proportion removed after 180 min increased from 63.17 to 85.49%, when the initial concentration decreased from 50 to 20 mg/L. After 180 min, the rate of adsorption almost approached equilibrium. Thus, 180 min was chosen as the reaction time in subsequent experiments.

The  $Q_e$  could be drawn from the results, when the concentration of Cr(VI) is 20 mg/L; the  $Q_e$  is about 16.61 mg/g, while  $Q_e$  of the Fe-modified AC prepared from *T. natans* husk is just 11.83 mg/g, when the concentration of Cr(VI) is 20 mg/L [11].

#### 3.3. Effect of temperature

Temperature is an important variable in most reactions, so the effect of temperature on Cr(VI) adsorption by AC was investigated. As shown in Fig. 4, the percentage of Cr(VI) removed in 3 h increased from 37.6 to 50.39% with the temperature increased from 20 to 40°C. Low temperature restrained the adsorption process, and there was minimal effect when the temperature reached a certain level. A possible reason for the lower adsorption at lower temperature was that the bonding between Cr(VI) ions and functional

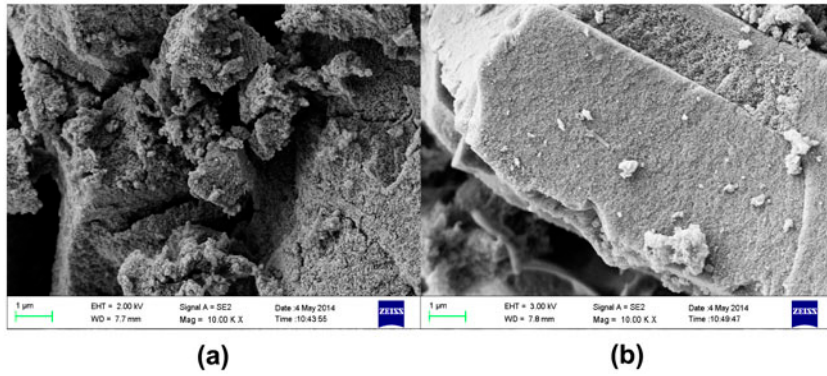


Fig. 1. SEM images of AC (a) before and (b) after Cr(VI) adsorption. AC content = 1.6 g/L; time = 3 h; initial concentration = 100 mg/L; and temperature = 25 °C.

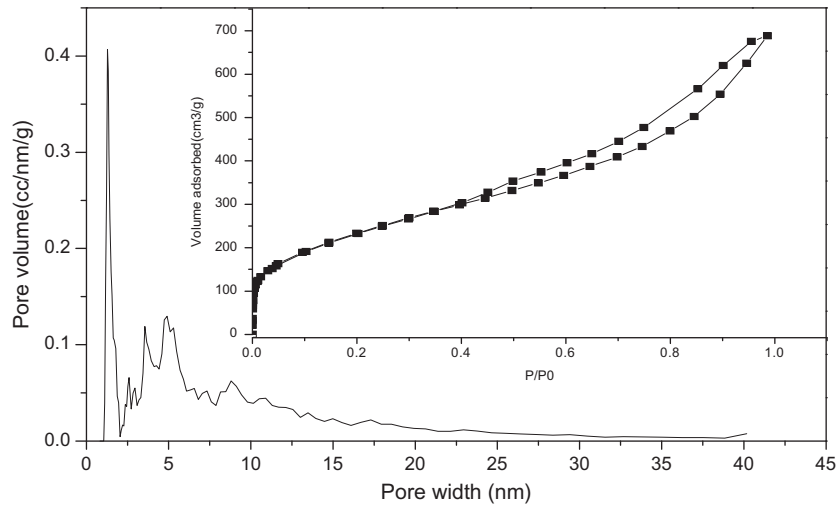


Fig. 2. Pore-size distribution of AC. The N<sub>2</sub> adsorption/desorption isotherms obtained for AC.

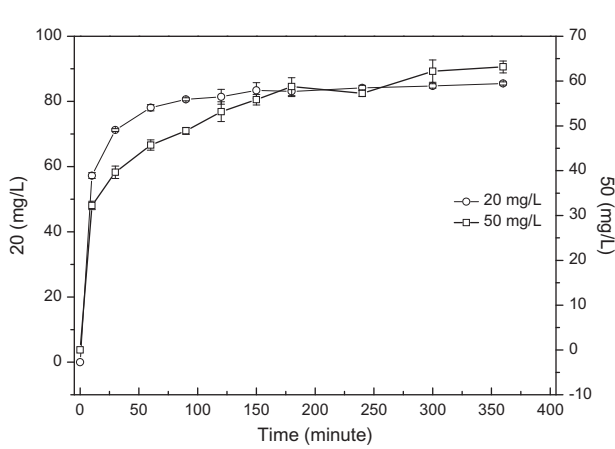


Fig. 3. Effect of contact time on percentage of Cr(VI) removed at initial concentrations of 20 and 50 mg/L. AC content = 1 g/L; temperature = 25 °C; time = 3 h; and the revolving speed = 180 r/min.

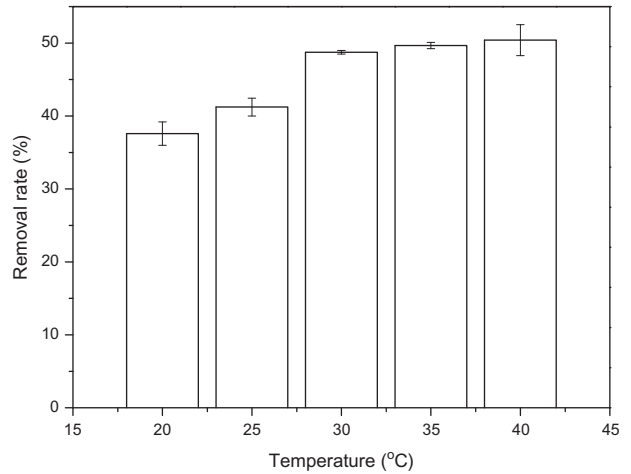


Fig. 4. Influence of temperature on Cr(VI) removal rate. AC content = 1.6 g/L; time = 3 h; initial concentration = 100 mg/L; and the revolving speed = 180 r/min.

groups on the AC surface was facilitated by a higher temperature. In subsequent experiments, 30°C was used as the experimental temperature.

### 3.4. Effect of initial solution pH

The initial solution pH is an important factor influencing metal sorption in aqueous solution because the surface properties of adsorbents, ionic state of functional groups, and metals, all depend on pH [23]. Fig. 5 reveals that the adsorption of Cr(VI) by AC was improved under acidic conditions. The Cr(VI) removal rate was high, when the pH of the initial solution was low. Conversely, under neutral or alkaline conditions, the adsorption of Cr(VI) by AC was inhibited. The pH of the solutions did not change after the adsorption process, so the Cr(VI) concentration had little effect on the solution pH. The removal rate increased sharply from about 57.25% to about 98.92% with the pH decreased from 6 to 1. The trend in adsorption capacity was similar to that of the removal rate, so acidic conditions were the best choice for the adsorption experiments.

Chromate can be present in various forms in the solution phase depending on pH and chromium concentration [24]:

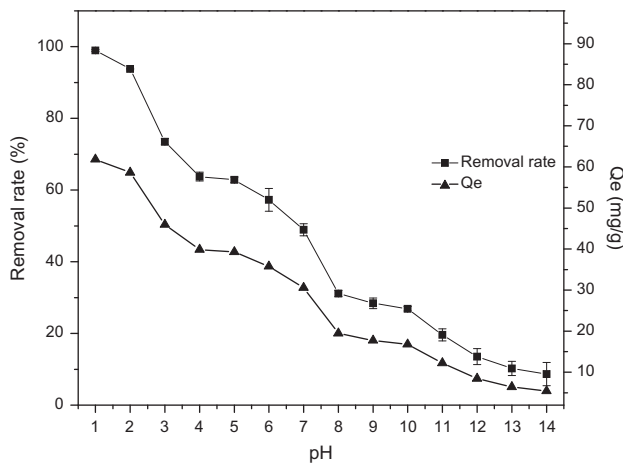
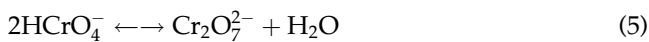
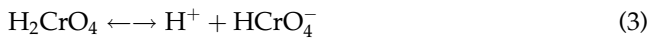


Fig. 5. Influence of solution pH on Cr(VI) removal rate and adsorption capacity. AC content = 1.6 g/L; temperature = 25°C; initial concentration = 100 mg/L; and the revolving speed = 180 r/min.

At a solution pH of 2–3, the predominant Cr(VI) species is  $\text{HCrO}_4^-$ , but as the pH increases, it forms  $\text{Cr}_2\text{O}_7^{2-}$  and  $\text{CrO}_4^{2-}$ .  $\text{HCrO}_4^-$  is more favorable for sorption than the other species because it has a low adsorption free energy [25].

### 3.5. Effect of AC content

To determine the optimum conditions for adsorption of Cr(VI) by AC, various AC contents (0.2–2 g/L) were used to adsorb Cr(VI) with a constant concentration of 100 mg/L. Fig. 6 reveals that the removal rate increased as the AC content increased from 0.2 to 1.2 g/L. About 98.62% of removal was achieved with 1.2 g/L of AC. Then the removal rate was stabilized. The removal efficiency reached as high as 99.26%. When the dose was increased further, the removal rate was basically unchanged but did decrease slightly. This is because the excess AC allowed a competing adsorption phenomenon to exist in the solution, which indirectly reduced adsorption efficiency.

Throughout the entire process, the adsorption capacity and maximum are the most important characteristics of the AC. Fig. 6 reveals that  $Q_e$  decreased dramatically above AC contents of 0.2 g/L. The most likely reason for this was that the AC contents below 0.2 g/L reached adsorption saturation (about 119 mg/g). When the AC content increased further, AC would adsorb relatively fewer Cr(VI) ions per amount added, and AC competed to adsorb Cr(VI) ions.

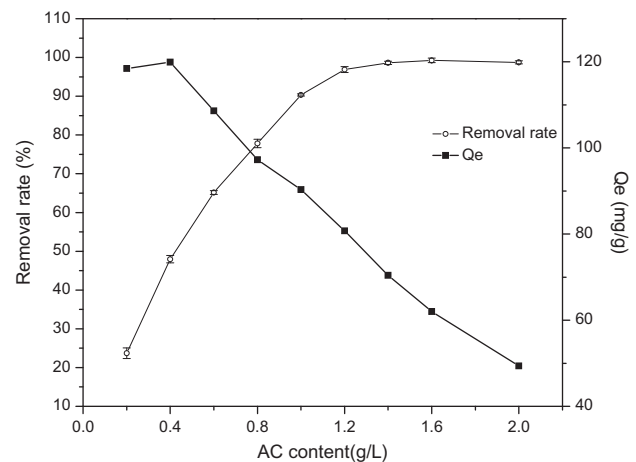


Fig. 6. Dependence of AC content on Cr(VI) removal rate and adsorption capacity. Temperature = 25°C; initial concentration = 100 mg/L; pH = 1; and the revolving speed = 180 r/min.



### 3.6. Effect of initial concentration

In this study, the maximum adsorption quantity of Cr(VI) was determined by changing the initial concentration of Cr(VI). With increasing concentrations of Cr(VI), the adsorption quantity changed as shown in Fig. 7,  $Q_e$  gradually increased as the initial concentration of Cr(VI) increased from 50 to 200 mg/L until it reached a maximum adsorption quantity of 149.06 mg/g, the peanut shells AC was about 95 mg/g when the concentration of Cr(VI) was 100 mg/L [26]. However, as the initial concentration of Cr(VI) was increased, the removal rate of Cr(VI) by AC rapidly decreased.

### 3.7. Orthogonal experiments

The three levels for different experimental conditions were confirmed through initial and single-factor experiments. The optimum condition was selected as the middle level, and then the same spacing on either side was used to determine the other levels, as listed in Table 1. The four factors considered were initial concentration, quantity of AC, solution pH, and temperature.

The results obtained of these orthogonal experiments are shown in Table 2. The optimal combination was pH = 1, initial Cr(VI) concentration = 80 mg/L, temperature = 303 K, and AC content = 1.6 g/L. Orthogonal testing revealed that the factors affecting Cr(VI) adsorption had the order of importance of solution pH > initial concentration > temperature > quantity of AC.

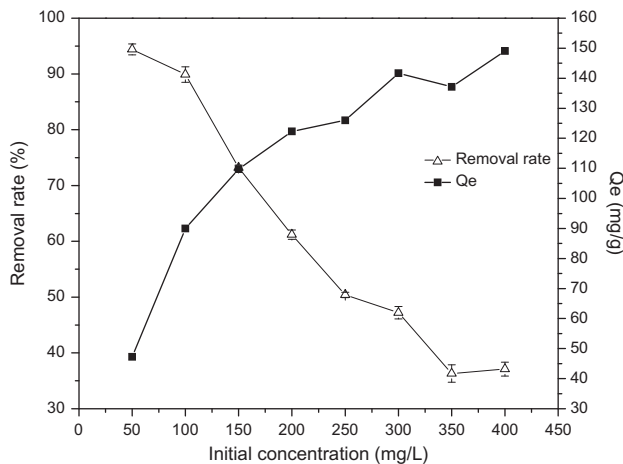


Fig. 7. Effect of the initial Cr(VI) concentration on the adsorption capacity of AC and removal rate. AC content = 1.6 g/L; temperature = 25°C; pH = 1; the revolving speed = 180 r/min; and time = 3 h.

According to the latest national standard requirements, the discharge standard for leather companies, leather and wool processing companies, and plating corporations is a maximum Cr(VI) concentration of 0.2 mg/L. The optimal combination of experimental conditions for Cr(VI) adsorption by AC could decrease the Cr(VI) concentration to 0.015 mg/L, which meets the required national standard.

### 3.8. Adsorption kinetics

The kinetics of the adsorption of Cr(VI) by AC considers three widely used models: the pseudo-first-order, pseudo-second-order model, and the rate of intraparticle diffusion were investigated. The linear form of the pseudo-first-order equation [27] can be expressed as

$$\ln(Q_e - Q_t) = \ln Q_e - k_1 t \quad (6)$$

where  $Q_e$  is the amount of Cr(VI) adsorbed at equilibrium (mg/g),  $Q_t$  is the amount of Cr(VI) adsorbed at time  $t$  (mg/g),  $k_1$  is the rate constant of the pseudo-first-order model (1/min), and  $t$  is time (min). The values of  $Q_e$  and  $k_1$  can be obtained from the intercept and slope of a plot of  $\ln(Q_e - Q_t)$  vs.  $t$ , respectively.

The linear form of the pseudo-second-order model equation [25] is given as follows:

$$t/Q_t = 1/k_2 Q_e^2 + t/Q_e \quad (7)$$

where  $Q_e$  is the amount of Cr(VI) adsorbed at equilibrium (mg/g),  $Q_t$  is the amount of Cr(VI) adsorbed at time  $t$  (mg/g),  $k_2$  is the rate constant of the pseudo-second-order model (g/(mg min)), and  $t$  is time (min). The parameters  $Q_e$  and  $k_2$  can be estimated from the slope and intercept of a plot of  $(t/Q_t)$  vs.  $t$ , respectively.

Adsorption of any metal ion from the aqueous phase onto porous materials proceeds by a multi-step process, and is usually controlled by either the film diffusion (external mass transfer) or the rate of intraparticle diffusion rate [28]. To identify the diffusion mechanism in the Cr(VI)/AC system, the intraparticle diffusion model is considered using the following equation [29]:

$$Q_t = k_p t^{0.5} + C \quad (8)$$

where  $k_p$  is the intraparticle diffusion rate constant (mg/(g min<sup>0.5</sup>)), and  $C$  is the intercept (mg/g).  $k_p$  and  $C$  can be obtained from a plot  $(Q_t)$  vs.  $t^{0.5}$ . Intraparticle

Table 1  
Levels of factors investigated to optimize adsorption conditions

pH	Temperature (°C)	Adsorbent dose (g/L)	Initial concentration (mg/L)
1	25	1.4	80
1.5	30	1.6	100
2	35	1.8	120

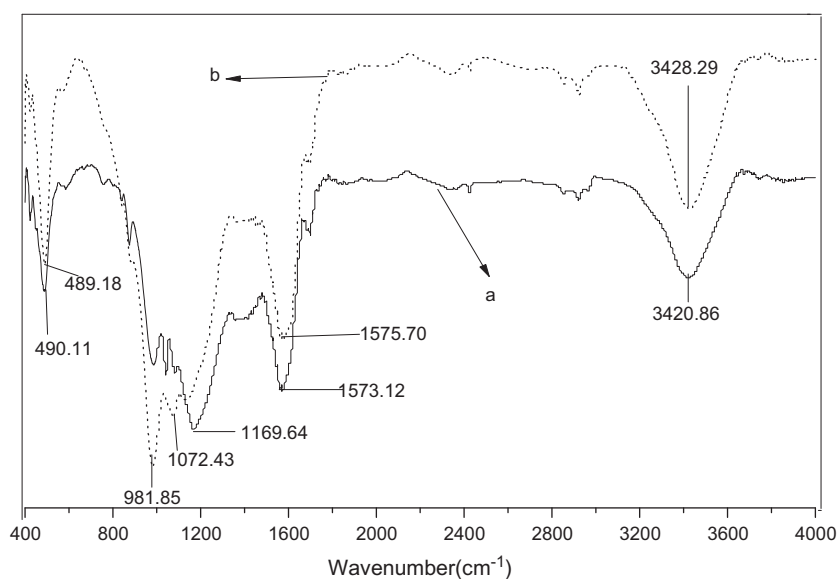


Fig. 8. FTIR spectra of AC (a) before and (b) after adsorption of Cr(VI).

Table 2  
Results of orthogonal experiments

	pH	Temperature (°C)	AC content (g/L)	Initial concentration (mg/L)	Removal efficiency (%)
1	1	25	1.4	80	99.28
2	1	30	1.6	100	99.97
3	1	35	1.8	120	99.97
4	1.5	25	1.6	120	95.79
5	1.5	30	1.8	80	99.89
6	1.5	35	1.4	100	99.45
7	2	25	1.8	100	95.32
8	2	30	1.4	120	88.52
9	2	35	1.6	80	99.68
k1	99.74	96.13	95.75	99.61	
k2	98.38	96.79	98.48	98.25	
k3	94.51	99.70	98.39	94.76	
R	5.23	3.57	2.73	4.85	

diffusion is the sole rate-limiting step if the plot of  $(Q_t)$  vs.  $t^{0.5}$  is a straight line that passes through the origin [30].

The best model to describe our Cr(VI)/AC system was determined using correlation coefficients ( $R^2$ ), together with a non-linear chi-square test analysis ( $X^2$ ), which was defined as [24]:

$$X^2 = \sum (Q_{\text{exp}} - Q_{\text{cal}})^2 / Q_{\text{cal}} \quad (9)$$

where  $Q_{\text{cal}}$  is the calculated amount of Cr(VI) adsorbed by AC (mg/g), and  $Q_{\text{exp}}$  is the experimental amount of Cr(VI) adsorbed by AC (mg/g).

A smaller  $X^2$  value means a better agreement between the values calculated from the model and the experimental data.

Table 3 lists all of the kinetic parameters, correlation coefficients, and  $X^2$  for the Cr(VI)/AC system. Compared with the pseudo-first-order model and the rate of intraparticle diffusion, the pseudo-second-order model fitted the experimental data quite well, and both  $R^2$  and  $X^2$  analyses supported this conclusion.  $R^2$  was 0.9994 and 0.9926 for the pseudo-second-order model. There was good agreement between  $Q_{\text{cal}}$  and  $Q_{\text{exp}}$ , and  $X^2$  for the pseudo-first-order model and the rate of intraparticle diffusion were higher than that determined for the pseudo-second-order model.  $C$  indicates the boundary thickness; the larger the  $C$  value is, the greater the effect of the boundary. The fit of the intraparticle diffusion rate was better for an AC content of 50 mg/L than for that at 20 mg/L. It meant that the lower concentration, the bigger the effect of the boundary.

Overall, the results suggest that adsorption of Cr(VI) by AC was not a first-order reaction, and

instead may be a pseudo-second-order reaction, based on the assumption that the rate-limiting step might be chemical sorption or chemisorption involving valence forces through the sharing or exchange of electrons between sorbent and sorbate [31]. Sharma and Forster reported that the kinetics of the sorption of Cr(VI) using peat, leaf mold, and granular AC is a pseudo-second-order reaction [32,33].

According to the experimental results and a good adsorption capacity compared with other low-cost AC adsorbents which is given in Table 4, AC derived from luffa sponge is a good adsorbent, it also provides a new method for Cr(VI) removal from aqueous waste.

### 3.9. FTIR analysis

FTIR spectra obtained for the AC before and after Cr(VI) adsorption were used to explore the adsorption mechanism further. Generally, the bands in the low-frequency region ( $400\text{--}1,000\text{ cm}^{-1}$ ) can be assigned to metal–oxygen and metal–hydroxyl vibrations [34]. The region between  $1,610$  and  $1,500\text{ cm}^{-1}$  is associated with C–C stretching in aromatic rings found on the lignin structure [35].

Fig. 8(b) reveals that the FTIR spectrum of the Cr(VI)-loaded contained bands centered at  $490.12$ ,  $1,072.43$ ,  $1,575.70$ , and  $3,428.29\text{ cm}^{-1}$ , which might correspond to the presence of M–O (metal–oxygen), C–O (acids, alcohols, phenols, and esters), C–C, and –OH (carboxyl and phenol functional groups), respectively [36]. The adsorption process also caused the intensity of the broad bands at  $490.12$ ,  $1,577.70$ , and  $3,428.29\text{ cm}^{-1}$  present in the FTIR spectrum of unreacted AC to increase. The intense peak at  $490.12\text{ cm}^{-1}$

Table 3  
Pseudo-first-order and pseudo-second-order models for the adsorption of Cr(VI) by AC

Kinetic model	Parameter (unit)	20 mg/L	50 mg/L
Pseudo-first-order	$k_1$ (1/min)	0.0094	0.0073
	$Q_{\text{cal}}$ (mg/g)	6.840084	21.3895
	$R^2$	0.9846	0.9804
	$X^2$	15.38824	5.359351
Pseudo-second-order	$k_2$ (g/(mg min))	0.002686	0.000709
	$Q_{\text{cal}}$ (mg/g)	17.82531	34.96503
	$R^2$	0.9994	0.9926
	$X^2$	0.029549	0.054516
Intraparticle diffusion	$k_p$ (mg/(g min <sup>0.5</sup> ))	1.4549	1.9295
	$C$ (mg/g)	62.312	29.743
	$R^2$	0.7288	0.9465
	$X^2$	32.80716	0.496129
$Q_{\text{exp}}$		17.09956	33.5844



Table 4  
Adsorption capacities of various low-cost AC adsorbents for Cr(VI)

Adsorbent	$Q_m$ (mg/g)	Sorbent content (g/L)	pH	Concentration (mg/L)	References
Fe-modified <i>Trapa natans</i> husk-activated carbon	11.83	1.5	6	20	[11]
Hazelnut shell-activated carbon	92	2.5	1	300	[37]
<i>Hevea brasiliensis</i> sawdust-activated carbon	63.99	1	2	200	[38]
<i>Terminalia arjuna</i> nuts-activated carbon	4.97	2	1	10	[39]
Luffa sponge-activated carbon	89.96	1	1	100	This work
	122.32	1		200	
	141.69	1		300	

for Cr(VI)-loaded AC can be attributed to the Cr–O bond vibration, confirming that the adsorbed Cr(VI) bonded with oxygen-containing functionalities on the sorbent surface [1]. The unreacted AC also had this peak at  $489.11\text{ cm}^{-1}$ , which might arise from other functional groups in this case. A new peak at  $981.85\text{ cm}^{-1}$  appeared after adsorption, which might be caused by binding of Cr(VI).

#### 4. Conclusion

The high surface area ( $834.13\text{ m}^2/\text{g}$ ) and pores (average size of  $5.17\text{ nm}$ ) of AC produced from luffa sponge resulted in excellent adsorption properties for Cr(VI). The optimal conditions for adsorption of Cr(VI) by AC were  $\text{pH} = 1$ , initial Cr(VI) concentration =  $80\text{ mg/L}$ ,  $T = 303\text{ K}$ , and AC content =  $1.6\text{ g/L}$ . Adsorption of Cr(VI) by AC was consistent with the pseudo-second-order model. Some functional groups such as C–O and O–H were formed on the carbon surface, which could then react with Cr(VI). The BET surface area and average pore size of the AC were  $834.13\text{ m}^2/\text{g}$  and  $5.17\text{ nm}$ , respectively. The maximum adsorption of Cr(VI) by AC was  $149.06\text{ mg/g}$ . The adsorption capacity was higher than other ACs from low-cost materials.

#### Acknowledgments

This work was supported by the Project funded by China Postdoctoral Science Foundation (No. 2014M551950), Promotive research fund for excellent young and middle-aged scientists of Shandong Province (No. BS2014HZ019), Major Science and Technology Program for Water Pollution Control and Treatment (2012ZX07203004), Major Science and Technology Program for Water Pollution Control and Treatment (2015ZX07203005), and Open Research Fund Program of Shandong Provincial Key Laboratory of Eco-Environmental Science for Yellow River Delta (Binzhou University) (No. 2013KFJJ01).

#### References

- [1] W.F. Liu, J. Zhang, C.L. Zhang, L. Ren, Preparation and evaluation of activated carbon-based iron-containing adsorbents for enhanced Cr(VI) removal: Mechanism study, *Chem. Eng. J.* 189–190 (2012) 295–302.
- [2] K.C. Lai, I.M. Lo, Removal of chromium (vi) by acid-washed zero-valent iron under various groundwater geochemistry conditions, *Environ. Sci. Technol.* 42 (2008) 1238–1244.
- [3] S.A. Martinez, M.G. Rodriguez, R. Aguilar, G. Soto, Removal of chromium hexavalent from rinsing chromating waters electrochemical reduction in a laboratory pilot plant, *Water Sci. Technol.* 49 (2004) 115–122.
- [4] N. Kongsricharoern, C. Polprasert, Chromium removal by a bipolar electro-chemical precipitation process, *Water Sci. Technol.* 34 (1996) 109–116.
- [5] C.A. Kozłowski, W. Walkowiak, Removal of chromium (VI) from aqueous solutions by polymer inclusion membranes, *Water Res.* 36 (2002) 4870–4876.
- [6] S. Rengaraj, K.H. Yeon, S.H. Moon, Removal of chromium from water and waste water by ion exchange resins, *J. Hazard. Mater.* 87 (2001) 273–287.
- [7] J. Fang, Z. Gu, D. Gang, C. Liu, E.S. Ilton, B. Deng, Cr(VI) removal from aqueous solution by activated carbon coated with quaternized poly(4-vinylpyridine), *Environ. Sci. Technol.* 41 (2007) 4748–4753.
- [8] A. Baran, E. Bıçak, S.H. Baysal, S. Onal, Comparative studies on the adsorption of Cr(VI) ions on to various sorbents, *Bioresour. Technol.* 98 (2006) 661–665.
- [9] Q. Gao, H. Liu, C. Cheng, K.Y. Li, J. Zhang, Ch.I. Zhang, Y.R. Li, Preparation and characterization of activated carbon from wool waste and the comparison of muffle furnace and microwave heating methods, *Powder Technol.* 249 (2013) 234–240.
- [10] Z.Z. Guo, X. Bian, J. Zhang, H. Liu, C. Cheng, C.L. Zhang, J. Wang, Activated carbons with well-developed microporosity prepared from *Phragmites australis* by potassium silicate activation, *J. Taiwan Inst. Chem. E.* 45 (2014) 2801–2804.
- [11] W.F. Liu, J. Zhang, C.L. Zhang, Y.F. Wang, Y. Li, Adsorptive removal of Cr(VI) by Fe-modified activated carbon prepared from *Trapa natans* husk, *Chem. Eng. J.* 162 (2010) 677–684.
- [12] Q.S. Liu, T. Zheng, P. Wang, L. Guo, Preparation and characterization of activated carbon from bamboo by microwave-induced phosphoric acid activation, *Ind. Crops Prod.* 31 (2010) 233–238.

- [13] W.T. Tsai, C.Y. Chang, M.C. Lin, S.F. Chien, H.F. Sun, M.F. Hsieh, Adsorption of acid dye onto activated carbons prepared from agricultural waste bagasse by  $ZnCl_2$  activation, *Chemosphere* 45(1) (2001) 51–58.
- [14] M.L. Martinez, M.M. Torres, C.A. Guzman, D.M. Maestri, Preparation and characteristics of activated carbon from olive stones and walnut shells, *Ind. Crops Prod.* 23 (2006) 23–28.
- [15] J. Hayashi, T. Horikawa, I. Takeda, K. Muroyama, F.N. Ani, Preparing activated carbon from various nutshells by chemical activation with  $K_2CO_3$ , *Carbon* 40 (2002) 2381–2386.
- [16] M. Momčilović, M. Purenović, A. Bojić, A. Zarubica, M. Randelović, Removal of lead(II) ions from aqueous solutions by adsorption onto pine cone activated carbon, *Desalination* 276 (2011) 53–59.
- [17] M. Wu, Q. Guo, G. Fu, Preparation and characteristics of medicinal activated carbon powders by  $CO_2$  activation of peanut shells, *Powder Technol.* 247 (2013) 188–196.
- [18] H. Deng, L. Yang, G. Tao, J. Dai, Preparation and characterization of activated carbon from cotton stalk by microwave assisted chemical activation—Application in methylene blue adsorption from aqueous solution, *J. Hazard. Mater.* 166 (2009) 1514–1521.
- [19] M. Kilic, E.A. Varol, A.E. Pütün, Adsorptive removal of phenol from aqueous solutions on activated carbon prepared from tobacco residues: Equilibrium, kinetics and thermodynamics, *J. Hazard. Mater.* 189 (2011) 397–403.
- [20] C. Cheng, J. Zhang, C.L. Zhang, H. Liu, W.f. Liu, Preparation and characterization of charcoal from feathers and its application in trimethoprim adsorption, *Desalin. Water Treat.* 52 (2014) 5401–5412.
- [21] H. Liu, J. Zhang, C.L. Zhang, N. Bao, C. Cheng, Activated carbons with well-developed microporosity and high surface acidity prepared from lotus stalks by organophosphorus compounds activations, *Carbon* 60 (2013) 289–291.
- [22] L. Wang, J. Zhang, R. Zhao, Y. Li, C. Li, C.L. Zhang, Adsorption of Pb(II) on activated carbon prepared from *Polygonum orientale* Linn: Kinetics, isotherms, pH, and ionic strength studies, *Bioresour. Technol.* 101 (2010) 5808–5814.
- [23] M.A. Hossain, H.H. Ngo, W.S. Guo, T.V. Nguyen, Palm oil fruit shells as biosorbent for copper removal from water and wastewater: Experiments and sorption models, *Bioresour. Technol.* 113 (2012) 97–110.
- [24] L.V.A. Gurgel, J.C.P. Melo, J.C. Lena, L.F. Gil, Adsorption of chromium (VI) ion from aqueous solution by succinylated mercerized cellulose functionalized with quaternary ammonium groups, *Bioresour. Technol.* 100 (2009) 3214–3220.
- [25] P. Yuan, M. Fan, D. Yang, H. He, D. Liu, A. Yuan, J. Zhu, T. Chen, Montmorillonite-supported magnetite nanoparticles for the removal of hexavalent chromium from aqueous solutions, *J. Hazard. Mater.* 166 (2009) 821–829.
- [26] L.J. Yu, B.S. Sun, T.G. Wang, Removal of chromium from aqueous solution by activated carbon made from peanut shells, *Chem. Eng.* 8 (2009) 8–12.
- [27] K. Periasamy, K. Srinivasan, P.R. Murugan, Studies on chromium (VI) removal by activated groundnut husk carbon, *J. Environ. Health* 33 (1991) 433–439.
- [28] R.L. Tseng, S.K. Tseng, Pore structure and adsorption performance of the KOH-activated carbons prepared from corncob, *J. Colloid Interface Sci.* 87 (2005) 428–437.
- [29] W.J. Weber, J.C. Morris, Kinetics of adsorption on carbon from solution, *J. Sanit. Eng. Div. Am. Soc. Civ. Eng.* 89 (1963) 31–59.
- [30] Ö. Gerc, A. Özcan, A.S. Özcan, H.F. Gerc, Preparation of activated carbon from a renewable bio-plant of *Euphorbia rigida* by  $H_2SO_4$  activation and its adsorption behavior in aqueous solutions, *Appl. Surf. Sci.* 253 (2007) 4843–4852.
- [31] Y.S. Ho, G. McKay, Pseudo-second order model for sorption processes, *Process Biochem.* 34 (1999) 451–465.
- [32] D.C. Sharma, C.F. Forster, Removal of hexavalent chromium using sphagnum moss peat, *Water Res.* 27 (1993) 120–1208.
- [33] D.C. Sharma, C.F. Forster, The treatment of chromium wastewaters using the sorptive potential of leaf mold, *Bioresour. Technol.* 49 (1994) 31–40.
- [34] Z. Ai, Y. Cheng, L. Zhang, J. Qiu, Efficient removal of Cr(VI) from aqueous solution with Fe@FeO core-shell nanowires, *Environ. Sci. Technol.* 42 (2008) 6955–6960.
- [35] C. Pasquali, H. Herrera, Pyrolysis of lignin and IR analysis of residues, *Thermochim. Acta* 293 (1997) 39–46.
- [36] H. Liu, J. Zhang, W.F. Liu, N. Bao, C. Cheng, C.L. Zhang, Preparation and characterization of activated charcoals from a new source: Feather, *Mater. Lett.* 87 (2012) 17–19.
- [37] M. Kobya, Removal of Cr(VI) from aqueous solutions by adsorption onto hazelnut shell activated carbon: Kinetic and equilibrium studies, *Bioresour. Technol.* 91 (2004) 317–321.
- [38] T. Karthikeyan, S. Rajgopal, L.R. Miranda, Chromium (VI) adsorption from aqueous solution by *Hevea brasiliensis* sawdust activated carbon, *J. Hazard. Mater.* 124 (2005) 192–199.
- [39] K. Mohanty, M. Jha, B.C. Meikap, M.N. Biswas, Removal of chromium (VI) from dilute aqueous solutions by activated carbon developed from *Terminalia arjuna* nuts activated with zinc chloride, *Chem. Eng. Sci.* 60 (2005) 3049–3059.